Cell, Vol. 96, 517–527, February 19, 1999, Copyright ©1999 by Cell Press

CLIP-170 Highlights Growing Microtubule Ends In Vivo

Franck Perez,* Georgios S. Diamantopoulos, Romaine Stalder, and Thomas E. Kreis†
Department of Cell Biology
Sciences III
University of Geneva
CH-1204 Geneva
Switzerland

Summary

A chimera with the green fluorescent protein (GFP) has been constructed to visualize the dynamic properties of the endosome-microtubule linker protein CLIP-170 (GFP-CLIP170). GFP-CLIP170 binds in stretches along a subset of microtubule ends. These fluorescent stretches appear to move with the growing tips of microtubules at 0.15–0.4 μm/s, comparable to microtubule elongation in vivo. Analysis of speckles along dynamic GFP-CLIP170 stretches suggests that CLIP-170 treadmills on growing microtubule ends, rather than being continuously transported toward these ends. Drugs affecting microtubule dynamics rapidly inhibit movement of GFP-CLIP170 dashes. We propose that GFP-CLIP170 highlights growing microtubule ends by specifically recognizing the structure of a segment of newly polymerized tubulin.

Introduction

Microtubules are dynamic polarized filaments essential for chromosome segregation during cell division (Hyman and Karsenti, 1996), for the regulation of intracellular membrane traffic by multiple specific molecular motor proteins (Goodson et al., 1997; Bloom and Goldstein, 1998; Hirokawa, 1998; Vale, 1998), and for the spatial arrangement of the cytoplasm in interphase (Cole and Lippincott-Schwartz, 1995). These specific functions of microtubules depend in part on their dynamic properties, which allow these cytoskeletal structures to rapidly explore the cytoplasmic space (Kirschner and Mitchison, 1986). In fibroblasts, most microtubules emanate from the microtubule organizing center (MTOC), and their fast-growing plus ends are usually directed toward the cell periphery. Microtubule plus ends display dynamic instability in vitro and in vivo (Mitchison and Kirschner, 1984; Sammak and Borisy, 1988; Walker et al., 1988). They alternate stochastically between phases of elongation and rapid shortening (Sammak and Borisy, 1988; Walker et al., 1988). The transition between growth and shrinkage most likely depends on the biochemical nature and structure of these ends and the presence and size of a tubulin "GTP cap" (Carlier and Pantaloni, 1981; Mitchison and Kirschner, 1984). Tubulin with bound GTP polymerizes at the plus ends, and, as microtubules grow, the GTP bound to the β subunits is hydrolyzed so that normally only a small segment of GTP-tubulin should remain (discussed by Caplow, 1992; Desai and Mitchison, 1997). This GTP cap is thought to be necessary for elongation of the polymer and to prevent microtubules from depolymerization, while hydrolysis of the nucleotide is a prerequisite for disassembly (Hyman et al., 1992). In addition, a structural cap has been observed at the growing microtubule ends in vitro. Morphological differences between growing and shrinking microtubule ends have been seen in vitro by electron microscopy (Simon and Salmon, 1990; Mandelkow et al., 1991). Furthermore, in vitro observation of polymorphic structures resembling sheets of tubulin at the growing ends of microtubules have lead to the proposal that microtubules grow as sheets of polymer, eventually closing up to form tubes (Chrétien et al., 1995). As proposed for the GTP cap, this structural cap may be necessary to sustain growth of microtubules and prevent their depolymerization.

Whether the same mechanism of polymerization also operates in vivo is unclear. It is likely that microtubule plus end dynamics depend on specific regulatory factors such as stathmin/Op18 (Belmont and Mitchison, 1996; Marklund et al., 1996), XMAP215/TOG1p (Gard and Kirschner, 1987; Charrasse et al., 1998), XKCM1 (Walczak et al., 1996), or XMAP310 (Andersen and Karsenti, 1997). CLIP-170, a microtubule binding protein that has been implicated in the attachment of endosomes to microtubules (Pierre et al., 1992), is so far the only microtubule binding protein that has been observed to colocalize with microtubule plus ends (Rickard and Kreis, 1990; Diamantopoulos et al., 1999). Binding of CLIP-170 to microtubules is regulated by phosphorylation (Rickard and Kreis, 1991), and it has been speculated that specific phosphorylation may be involved in the targeting of CLIP-170 to microtubule plus ends (Rickard and Kreis, 1996). Interestingly, CLIP-170 may also interact with the dynactin complex (C. Valetti et al., submitted), an activator of cytoplasmic dynein (Schroer and Sheetz, 1991) that contains a subunit, p150^{Glued}, which has one CLIP-170-related microtubule binding domain per molecule (Holzbaur et al., 1991; Pierre et al., 1992; Waterman-Storer et al., 1995a). CLIP-170 may thus play a role in regulating the dynamic properties of microtubule plus ends or may be a capturing device to clip peripheral organelles to microtubules before it hands them over, perhaps via dynactin, to the microtubule minus end–directed motor protein cytoplasmic dynein. To this end, the functional significance of the microtubule plus end localization of CLIP-170 is unclear.

To further characterize the function of CLIP-170, we have generated a chimera of CLIP-170 with green fluorescent protein (GFP-CLIP170) and visualized its dynamic properties using time-lapse fluorescence microscopy of Vero cells transiently expressing GFP-CLIP170. The striking features of GFP-CLIP170 dynamics in vivo suggest that it "treadmills" on the growing microtubule plus ends and that this activity thus follows microtubule ends toward the cell periphery.

*To whom correspondence should be addressed (e-mail: franck.perez@cellbio.unige.ch).
† This article is dedicated to the memory of Thomas E. Kreis.

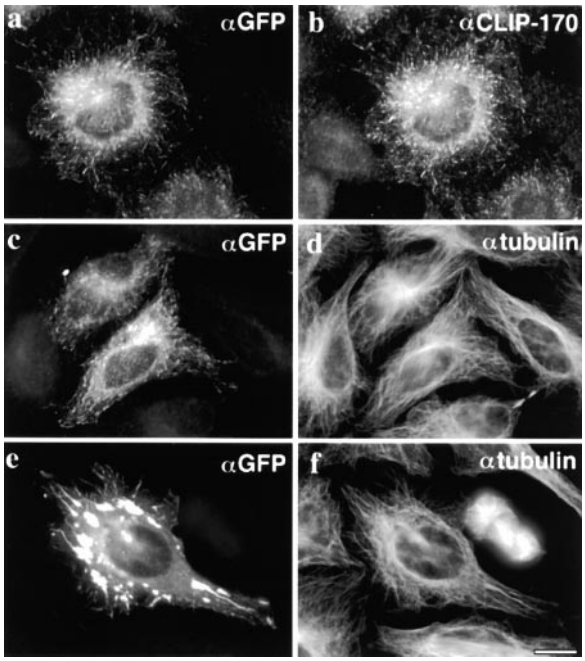

Figure 1. Transiently Expressed GFP-CLIP170 Is Localized to Microtubule Plus Ends in HeLa Cells

HeLa cells were transfected with the plasmid encoding GFP-CLIP170, fixed 24 hr later, and labeled by indirect double immunofluorescence using polyclonal rabbit antibodies against GFP (a, c, and e) and murine monoclonal antibodies against CLIP-170 (b) or tubulin (d and f), followed by fluorescein- and rhodamine-labeled antibodies against rabbit and mouse IgG, respectively. At low expression levels (a–d), GFP-CLIP170 is, like the endogenous protein, associated with stretches of variable length of a subset of peripheral microtubule ends. At higher expression levels (e and f), we find the recombinant protein in large aggregates at the bases of microtubule bundles. Scale bar, 10 μm.

Results

We have generated a fluorescent CLIP-170 to visualize its dynamic distribution in vivo and to better understand its potential role in microtubule dynamic properties and membrane traffic.

Transiently Expressed GFP-CLIP170 Is Associated with Microtubule Plus Ends

We have constructed a fusion protein between human CLIP-170 (Pierre et al., 1992) and a bright, red-shifted GFP mutant (Cormack et al., 1996). GFP was attached to the N terminus of CLIP-170, since epitope tagging of the protein at this site appeared not to interfere with CLIP-170 function (Pierre et al., 1994). Multiple lines of evidence suggest that full-length CLIP-170 is tagged with GFP, and that it indeed behaves like the endogenous protein. Expressed GFP-CLIP170 is recognized by polyclonal antibodies detecting an epitope in the coiled-coil region, as well as by a monoclonal antibody (2D6) reacting with the C-terminal domain of the protein (data not shown). Since GFP has been inserted at the N terminus of the protein, we conclude that an intact CLIP-170 fusion protein with GFP is expressed. Moreover, a protein of ~200 kDa could be immunoprecipitated from cells transiently expressing GFP-CLIP170 with antibodies directed against GFP or CLIP-170 (data not shown). We also tested the two functional activities of the N- and C-terminal domains of the chimeric protein. Like the wild-type protein (Pierre et al., 1992), in vitro–translated GFP-CLIP170 binds to microtubules in vitro (data not shown). When transiently expressed at low levels in HeLa (Figure 1) or Vero cells (data not shown), GFP-CLIP170 localizes in stretches of various lengths along the distal (plus) ends of a subset of microtubules (Figures 1a and 1c), as has been observed for the endogenous (Rickard and Kreis, 1990) or transiently expressed Myc-tagged protein (Pierre et al., 1994). Thus, the microtubule binding N-terminal domain of CLIP-170 is not significantly perturbed by GFP. Furthermore, upon overexpression of the chimeric protein, it binds along the length of microtubules, induces bundling of microtubules, and eventually accumulates in large aggregates (Figure 1e), identical to what has been observed with overexpressed wild-type or epitope-tagged CLIP-170 (Pierre et al., 1994). Accumulation of CLIP-170 into such patches depends on an intact C-terminal domain, corroborating that a functionally intact chimera is expressed. Based on these data, we conclude that GFP-CLIP170 can faithfully trace the dynamic properties of the endogenous protein.

GFP-CLIP170 Binds to Growing Microtubule Ends In Vivo

To characterize the dynamic properties of GFP-CLIP170, we have visualized the fluorescent protein in vivo. We have chosen the fibroblastic Vero cells for these experiments, since they have most of their microtubules nucleated by the juxtanuclear MTOC. Cells were microinjected into their nuclei with pCB6-GFP-CLIP170 DNA (50 ng/μl) and observed with a cooled CCD camera under the fluorescence microscope 3 hr later. To avoid potential problems of interference with normal CLIP-170 function due to overexpression of the protein, we have studied only selected cells expressing minimal detectable levels of fluorescent CLIP-170. The distribution of GFP-CLIP170 is virtually identical to that of the endogenous protein in these cells, and no aggregation of fluorescence into patches nor microtubule bundling can be observed. In addition, microtubule dynamic properties appear not to be significantly altered in these transfected cells, since the rate of microtubule growth is in accord with previously published values (see below). The dynamic properties of GFP-CLIP170 are striking: it moves in comet-like dashes on linear trajectories from a juxtanuclear site (the MTOC) toward the cell periphery in a manner resembling a "cellular firework" (Figure 2). New patches constantly form, more often around the MTOC but sometimes also randomly throughout the cytoplasm, and the movement of the vast majority is directed toward the periphery in the Vero cells (Figures 2 and 3). The movement of fluorescent dashes is often uninterrupted and can last for up to more than a minute before the signals disappear (open arrows in Figure 2). Usually, the dashes slow down, shorten, and then fade out (this often occurs upon reaching the cell periphery), but occasionally stretches of GFP-CLIP170 fluorescence that have stopped moving can also fade out

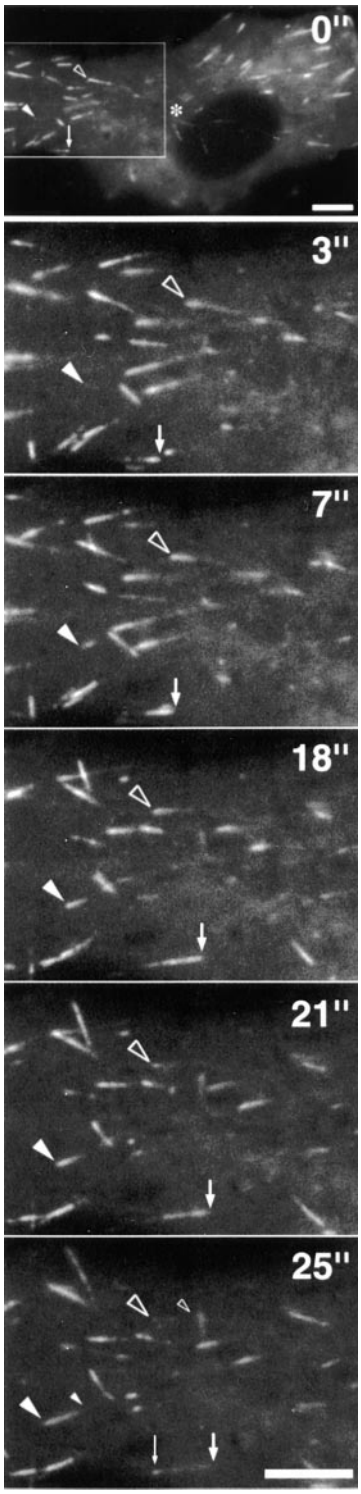

Figure 2. GFP-CLIP170 Transiently Expressed in Vero Cells Moves in Dashes from the MTOC toward the Cell Periphery

Vero cells were transfected by microinjection into the nucleus with pCB6-GFP-CLIP170 DNA. GFP-CLIP170 was visualized ~3 hr later by digital fluorescence microscopy in cells kept at 37°C in Hank's/BSA. Images of the distribution of GFP-CLIP170 were acquired every 3–5 s (as indicated). The top image shows most of the Vero cell, of which a flat part at the periphery was enlarged (boxed region) to visualize the dynamic properties of GFP-CLIP170. The likely position of the MTOC of this cell is indicated by an asterisk. Dashes of GFP-CLIP170 usually build up in the centrosomal region and move linearly toward the cell periphery, where they disappear. Examples of moving GFP-CLIP170 dashes are indicated (the bigger markers depicting the position of the front and the smaller ones the tip of its position at the beginning of the recording period). The closed arrowhead indicates a newly formed GFP-CLIP170 patch moving toward the periphery, the open arrowhead indicates a disappearing GFP-CLIP170 patch, and the arrow indicates one of the rare GFP-CLIP170 patches moving inward. Scale bar, 10 μm. The QuickTime (1.5 MB) movie from which these images were taken can be found at http://www.cell.com/cgi/content/full/96/4/517/DC1/1 (this movie has been accelerated 30 times).

evenly along their length (see, for example, the stretch indicated with arrows in Figure 2). Velocities of movement along one trajectory appear to be predominantly monotonous, with eventual phases of slowing down or pauses. Importantly, we have never observed dashes moving backward along their original tracks. Occasionally, intense dots of GFP-CLIP170 can be observed, jiggling around at random sites in the cytoplasm, which either disappear after a certain time or generate a new fluorescent dash (see, for example, Figure 3A).

Fluorescent dashes can measure up to 5 μm in length; they are not uniform in size and intensities and they are usually asymmetric, with rather sharp and brightly fluorescent fronts, fading out at their rear ends (see, for example, the patches indicated in Figure 2). Thus, movement appears to be generated by rapid recruitment of fluorescence to the tip of the stretches and loss of GFP-CLIP170 at their tails. The velocities of moving GFP-CLIP170 dashes were quantified by tracking of their bright tips (Figure 3). The average calculated speed (Figure 3B) is 0.21 ± 0.05 μm/s (n = 59 microtubules, data from 6 cells), and individual velocities can vary within individual cells between 0.15 and 0.4 μm/s (Figure 3B and data not shown). These velocities appear not to vary significantly at different (low) levels of expressed GFP-CLIP170. The few inwardly directed dashes move with the same average velocities. Interestingly, the monomeric microtubule binding head domain (H1) of the protein (GFP-H-CLIP170), or a fragment of CLIP-170 lacking the C-terminal tail domain (GFP-CLIP170-ΔT), show virtually identical dynamic properties to the intact fluorescent protein; their average velocities of movement are 0.22 ± 0.07 μm/s (n = 62 microtubules, 6 cells) and 0.24 ± 0.05 μm/s (n = 20 microtubules, 2 cells). As reported earlier, CLIP-170 mutants lacking an intact C terminus do not aggregate into the large patches observed with overexpressed intact protein (see also Pierre et al., 1994). However, GFP-tagged H1 and CLIP-170-ΔT, like the intact GFP-CLIP170, clearly label dashes on microtubule plus ends at low expression levels. Thus, the microtubule binding domain is necessary and sufficient for defining the dynamic properties of CLIP-170.

The dynamic properties of GFP-CLIP170 are virtually identical to the dynamic properties of growing microtubules in vivo; depending on the cell type investigated, microtubule elongation has been measured to be 3–20 μm/min (i.e., 0.05–0.35 μm/s; Cassimeris et al., 1988; Sammak and Borisy, 1988; Dhamodharan and Wadsworth, 1995). To further investigate the correlation of

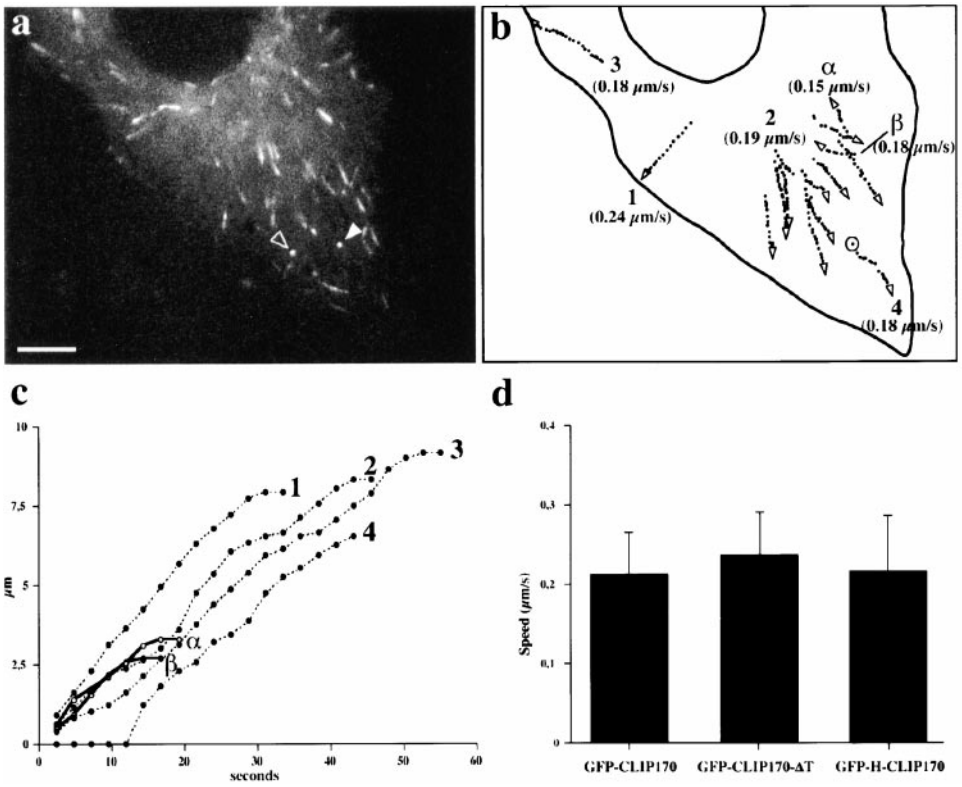

Figure 3. Quantification of the Movement of GFP-CLIP170-Positive Structures

GFP-CLIP170 was visualized in Vero cells as described in the legend to Figure 2, and the velocities of fluorescent dashes containing GFP-CLIP170 were measured. The cell shown in (a) is a typical example in which dashes that could be distinguished unambiguously have been tracked (b); dots represent the position of GFP-CLIP170 on consecutive frames taken at 2.4 s intervals. The profiles of their velocities of movement have been determined (c). Velocities were determined by tracking the tip at the front of the comet-like structure and measuring the movement as a function of time. The average speed of movement of some individual dashes is indicated (b). GFP-CLIP170 dashes moving toward the periphery are indicated with numbers, and those moving toward the interior of the cell with Greek letters. The circled dot indicates a GFP-CLIP170-labeled dash that stayed immobile for >20 s before it started moving (closed arrowhead in [a]); the dash indicated with an open arrowhead in (a) eventually disappeared. The mean velocities of movement of dashes of GFP-CLIP170 (0.21 ± 0.05, 59 dashes tracked in 6 cells), GFP-CLIP170-ΔT (0.24 ± 0.05, 20 dashes tracked in 2 cells), and GFP-H-CLIP170 (0.22 ± 0.07, 62 dashes tracked in 6 cells) have been determined in Vero cells transiently expressing these constructs. No significant differences could be detected between the intact and fragmented fluorescent proteins. Scale bar, 10 μm. The QuickTime (1.9 MB) movie from which these images were taken can be found at http://www.cell.com/cgi/content/full/96/4/517/DC1/2 (this movie has been accelerated 30 times).

GFP-CLIP170 and microtubule dynamics, we have covisualized GFP-CLIP170 with rhodamine-labeled tubulin (Rh-tubulin). Rh-tubulin was microinjected into Vero cells, and the same cells were injected 24 hr later with pCB6-GFP-CLIP170 DNA. Three more hours later, GFP-CLIP170 and rhodamine-labeled microtubules were visualized. The high density of microtubules in most of the cells investigated complicated or precluded a reliable analysis of microtubule growth and GFP-CLIP170 movement. In a few cells, however, we could unambiguously resolve and covisualize the dynamic properties of both structures. In the example shown, a presumably growing microtubule can be followed underneath the nucleus (Figure 4). Comparison of the movement of GFP-CLIP170 fluorescence with growth of that particular microtubule revealed that the movement of the CLIP-170 dash coincides closely with the advancing end of a microtubule. Interestingly, when microtubule growth slows down, the GFP-CLIP170 dash shortens (see 24′′ frame in Figure 4; see also Figure 6). Furthermore, a shrinking microtubule has been observed in the same area of that cell. No GFP-CLIP170 is found at the dynamic tip of this retracting microtubule (see closed arrows in Figure 4); however, upon rescue from depolymerization, a distinct patch of GFP-CLIP170 reappears on that microtubule, which then appears to regrow (see open arrow on last frames in Figure 4). Fluorescent CLIP-170 stretches appear to be exclusively associated with growing microtubule ends; most of the microtubules in a field are usually not labeled, and we have so far never observed additional stretches along microtubules distal from their plus ends. These data strongly suggest that CLIP-170 binds only to the growing microtubule ends.

Localization of CLIP-170 to growing microtubule plus ends could either occur by continuous movement to the growing tip (transport) or by association with the new polymer and release from the more distal, older part of the microtubule (treadmilling). Careful analysis of dynamic GFP-CLIP170 comets revealed inhomogeneities of fluorescence intensities (“speckles;” see also Waterman-Storer and Salmon, 1997, 1998a) along the structure. These speckles remained immobile as the dashes appeared to move with the growing microtubule ends (Figure 5), suggesting that CLIP-170 is not continuously

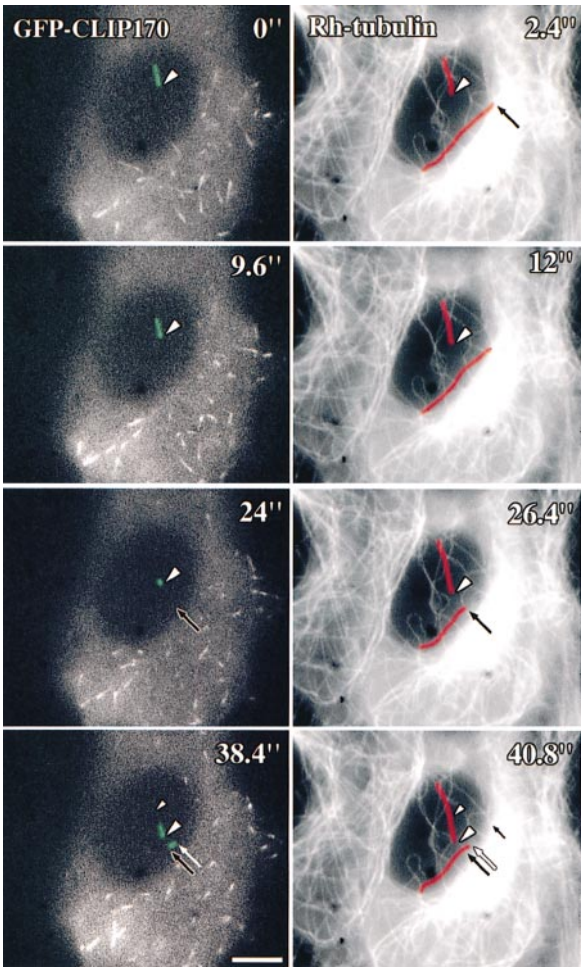

Figure 4. Movement of GFP-CLIP170 Dashes Coincides with the Growing Tips of Microtubules

Rh-tubulin was microinjected into the cytoplasm of Vero cells 24 hr before nuclear microinjection of the same cells with the GFP-CLIP170 DNA. The dynamic properties of Rh-tubulin and GFP-CLIP170 were recorded 3 hr later as described in the legend to Figure 2. Times of image acquisition are indicated, and the gap between recording of the green fluorescent CLIP-170 and the red fluorescent tubulin is 2.4 s. Two clearly visible dynamic microtubules are highlighted (red overlaid color) together with their associated GFP-CLIP170 dashes (green overlaid color). The tip of the growing microtubule underneath the middle of the nucleus is indicated with an arrowhead (in the last frame, small and large arrowheads indicate the position of elongation at the beginning and end of the recorded period, respectively). It is noteworthy that the GFP-CLIP170 structure associated with the rapidly growing microtubule is dash-like but changes to a rather dotty structure as microtubule growth slows down. Furthermore, no GFP-CLIP170 labeling is found along the length of other distinct microtubules in this field. The other microtubule indicated at the right border of the nucleus initially depolymerizes (follow the black arrows) before it is rescued from shrinking and appears to regrow (white arrow); as it is rescued from depolymerization and apparent growth is resumed, a distinct stretch of GFP-CLIP170 (white arrow) colocalizes with the tip of this microtubule. Scale bar, 10 μm. The QuickTime (0.75 MB) movie from which these images were taken can be found at http://www.cell.com/cgi/content/full/96/4/517/DC1/3 (this movie has been accelerated 30 times).

actively transported along the polymer toward the microtubule end but rather treadmills on that peripheral segment of growing microtubule. We analyzed further

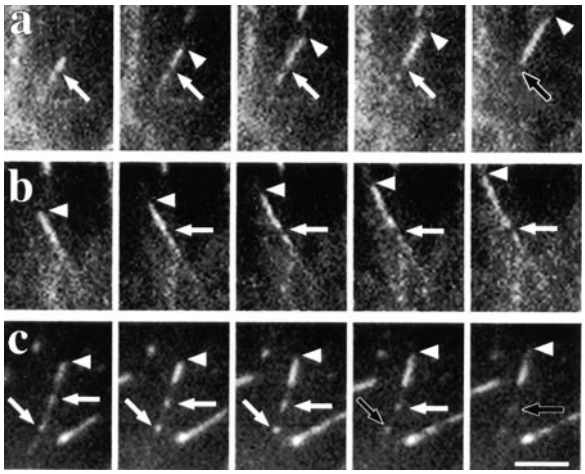

Figure 5. CLIP-170 Treadmills on Stretches of Growing Microtubule Ends

Inhomogeneities (speckles) of the fluorescence signals along GFP-CLIP170-labeled dashes have been followed as internal markers to reveal the overall dynamic properties of these structures. Arrows indicate darker (a and b) or brighter (c) speckles, which we have used as landmarks to visualize movement of the dashes relative to the front tips (arrowheads). No sliding of the speckles could be observed, while the tips of the stretches were either extending (a and b) or fading out (c). The black arrows indicate disappearance of speckles. Images were recorded at 2.8 s intervals. Scale bar, 3 μm.

the kinetics of CLIP-170 addition and loss and compared it with the variation of stretch size (Figure 6; see Experimental Procedures). The mean stretch size was calculated to be 2.23 ± 0.90 μm (131 time points for 9 microtubules). Very similar extension (0.288 ± 0.143 μm/s, 131 time points for 9 microtubules) and detachment (0.269 ± 0.176 μm/s, 123 time points for 7 microtubules) speeds were observed. The calculated standard error reflects the large variation in kinetics observed in between particular time points. The kinetics of extension of CLIP-170-positive stretches indeed shows a very irregular pattern. It alternates rapidly between phases of fast extension and pause or slow growth. Interestingly, we did not observe any GFP-CLIP170 stretch pausing for more than 10 s. In addition, this analysis revealed that the kinetics of detachment of GFP-CLIP170 from the older part of the polymer is also very irregular in its rates, showing phases of fast and slow detachment of the protein. This suggests that treadmilling of CLIP-170 at the plus ends of microtubules is controlled by the balance between variable rates of attachment and of detachment, and that regulatory—or stochastic—steps may take place for both of these events.

Drugs Perturbing Microtubule Dynamic Properties Affect Targeting of GFP-CLIP170 to Microtubule Ends

Since GFP-CLIP170 appears to associate exclusively and specifically with growing microtubule ends, we investigated whether modification of microtubule dynamic properties with nocodazole or taxol (Wilson and Jordan, 1994) affects its dynamic distribution. Low and high doses of either of these two microtubule poisons resulted in a rapid and dramatic redistribution of GFP-CLIP170 (Figure 7); virtually identical effects were also

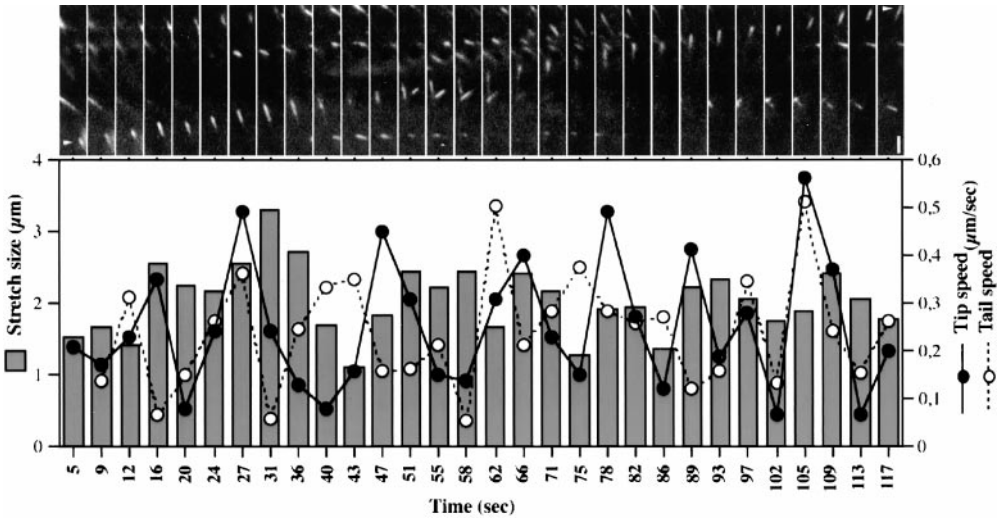

Figure 6. Treadmilling of GFP-CLIP170 Is Controlled by Variable Extension and Detachment Rates

GFP-CLIP170 was visualized in Vero cells as described in the legend to Figure 2, and the displacements of the tip and the tail of the fluorescent dash were measured as a function of time. The top panel shows the GFP-CLIP170-positive stretch that was followed every 3–5 s during 117 s (arrowheads point its position at the beginning and at the end of the recording period). The successive stretch lengths have been represented on the graph below (gray bars), which shows that they are variable and oscillate between 1.1 and 3.3 μm. The corresponding speed of displacement of the tip (closed circle) and the tail (open circle) of the GFP-CLIP170-positive structures showed that both the elongation and the detachment rate are variable and determine the extent of CLIP-170 treadmilling. Scale bar, 3 μm. The QuickTime movie from which these images were taken can be found at http://www.cell.com/cgi/content/full/96/4/517/DC1/4 (this movie has been accelerated 30 times).

observed on the endogenous protein (data not shown). Nocodazole (10 μM) removes GFP-CLIP170 from microtubule ends within a few seconds, while under the same conditions no significant relocation of the transiently expressed microtubule binding domain of MAP4 tagged with GFP (GFP-MAP4m) could be detected (Figure 7A). Lower doses of nocodazole (0.2 μM, Figure 7B; 0.05 μM, data not shown) have the same, albeit a somewhat slower, effect (~30 s). Interestingly and consistently, a faint but significant labeling of GFP-CLIP170 along the entire microtubule length appears later, within minutes in the presence of nocodazole (see arrowheads in Figures 7A and 7B). This finding is consistent with previous data, in which we have shown that nocodazole induces dephosphorylation of CLIP-170 (Rickard and Kreis, 1991), and our hypothesis that phosphorylation plays an important role in targeting of CLIP-170 to microtubule plus ends (Rickard and Kreis, 1996). At later time points (>30 min), when microtubules are almost completely depolymerized, GFP-CLIP170 accumulates, as previously observed, along the length of the few remaining nocodazole-resistant microtubules (data not shown; Rickard and Kreis, 1990). This nocodazole-induced relocation of GFP-CLIP170 is fully reversible (Figure 7B). Upon washout of the drug, GFP-CLIP170 reassociates with growing microtubule ends within <1 min. This result also strongly suggests that eventual photodamage due to visualization of GFP fluorescence over several minutes in the live cells is only marginal in our experiments.

Treatment of cells with taxol (at concentrations ranging from 0.2 to 10 μM) had a similar, albeit less rapid (~1 min), effect on the dynamic distribution of GFP-CLIP170; dashes of fluorescence disappear, leaving behind a small number of fluorescent dots (Figure 7C), reminiscent of those that can occasionally be observed in normal cells (see Figure 3A). This result is particularly remarkable, since taxol is known for its microtubule polymerization stimulatory activity. That GFP-CLIP170 does not bind to taxol-induced microtubules in vivo (even at low concentrations of the drug) may suggest a different conformation of the taxol and normally assembled (GTP-) tubulin polymer (see also Discussion). No comparable effect has been observed under the same conditions on the dynamic properties and the distribution of GFP-MAP4m (data not shown). Taken together, these experiments again suggest that localization of CLIP-170 depends on microtubule dynamics. Poisoning or altering microtubule growth with either nocodazole or taxol immediately abolishes rebinding of CLIP-170 to microtubule plus ends.

Discussion

We have tagged CLIP-170 with GFP to visualize its dynamic properties in vivo. Transiently expressed GFP-CLIP170 behaves like the endogenous protein in cells. It colocalizes with microtubule plus ends and accumulates in patchy, aggregated structures upon overexpression, suggesting that both the microtubule binding domain, as well as its putative membrane binding site, retained their functional activity in the chimera. We show here that GFP-CLIP170 visualizes the dynamic properties of growing microtubule ends. Poisoning microtubule polymerization with nocodazole or taxol rapidly removes the fluorescent protein from microtubule plus ends.

The specific localization of CLIP-170 to a subset of microtubule plus ends is so far unique. While localization near microtubule plus ends has also been observed for tea1 from *Schizosaccaromyces pombe* (Mata and Nurse, 1997) and the adenomatous polyposis tumor coli

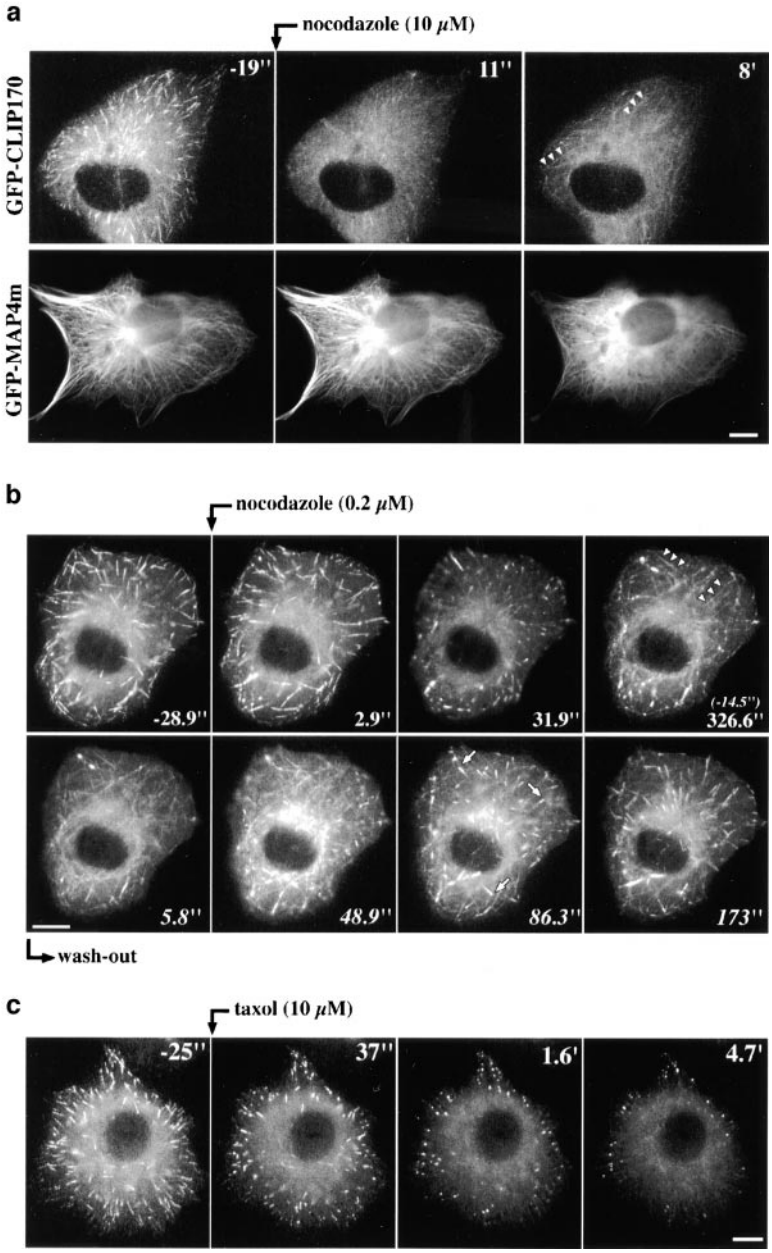

Figure 7. Alteration of Microtubule Dynamics by Drug Treatment of Cells Rapidly Affects GFP-CLIP170 Localization

Vero cells transfected with GFP-CLIP170 or the GFP-tagged microtubule binding domain of MAP4 (GFP-MAP4m) were treated with different concentrations of nocodazole (a and b) or taxol (c). The dynamic properties of the fluorescent proteins were followed in these cells as described in the legend to Figure 2; times before, during, or after washout of the drugs are indicated on the photographs. Treatment of cells with 10 μM nocodazole leads to an almost immediate removal of moving GFP-CLIP170 dashes from microtubule plus ends (a), while the overall microtubule pattern remains virtually unchanged during the first ~20 s of drug treatment, as visualized with GFP-MAP4m. At later time points of nocodazole treatment, GFP-CLIP170 can be found on remaining microtubules along their entire lengths (arrowheads at 8′). This effect of nocodazole on GFP-CLIP170 dynamics is reversible (b). Lower concentrations of nocodazole (0.2 μM) have been used to improve the rapid removal of the drug from the culture medium as the cells were being observed by fluorescence microscopy. Even at this low nocodazole concentration, dashes of GFP-CLIP170 disappeared within <1 min, and GFP-CLIP170 relocalized to a pattern labeling the entire length of microtubules (arrowheads at 326.6′′). Cells regained rapidly (~2 min) a normal dynamic behavior of GFP-CLIP170 upon removal of the drug (moving fluorescent dashes are indicated by arrows). In (c), treatment of cells with taxol (10 μM) rapidly (~1 min) inhibited the movement of most GFP-CLIP170 stretches, leaving behind, at later time points (>4 min), dots preferentially located at the cell periphery. Scale bar, 10 μm. The QuickTime movies from which these images were taken can be found at the following locations: for Figure 7a, http://www.cell.com/cgi/content/full/96/4/517/DC1/5 (4.8 MB) and http://www.cell.com/cgi/content/full/96/4/517/DC1/6 (3.1 MB); for Figure 7b, http://www.cell.com/cgi/content/full/96/4/517/DC1/7 (4.1 MB); and for Figure 7c, http://www.cell.com/cgi/content/full/96/4/517/DC1/8 (1.5 MB).

suppressor protein (APC; Näthke et al., 1996) and has been suggested for XMAP215/TOG1p (Vasquez et al., 1994; Charrasse et al., 1998), of all the microtubule binding proteins known, CLIP-170 is so far the only one for which such a precise dynamic regulation of microtubule plus end binding has been shown. The dynamic properties of GFP-CLIP170, in fact, coincide with those of polymerizing microtubule ends visualized with microinjected Rh-tubulin, strongly suggesting that CLIP-170 is targeted to the subset of growing microtubules. In addition, we have so far never observed growing microtubule ends devoid of CLIP-170. This suggests that all polymerizing microtubules are positive for CLIP-170, which is also supported by the observation that CLIP-170 labeled >90% of the microtubule ends that have incorporated microinjected biotinylated tubulin over a period of <1 min. In comparison, <40% of the supposedly older microtubule ends that did not elongate during the few seconds following microinjection of biotin-tubulin were positive for CLIP-170 (Diamantopoulos et al., 1999). Some paused microtubule ends may be positive for CLIP-170, but we observed that in this case the staining for CLIP-170 seems more dot-like than extended (Figure 3A and data not shown). That the association of CLIP-170 to elongating microtubules is strongly linked to polymerization of tubulin is further supported by the observation that certain drugs (i.e., nocodazole, taxol), known to modify the dynamic properties of growing microtubule ends, dramatically affect the dynamic distribution of CLIP-170.

Both binding of GFP-CLIP170 to the tip of growing microtubules, as well as its dissociation from the rear

end of the stretch along the polymer, are rapid and probably responsible for the comet-like shape of the fluorescent dashes. The pattern of movement of GFP-CLIP170 in the cytoplasm is reminiscent of a firework originating from the juxtanuclear region of the MTOC. Its velocities of movement (0.15–0.4 μm/s) are comparable to the published values for microtubule growth in vivo (0.05–0.35 μm/s; Cassimeris et al., 1988; Sammak and Borisy, 1988; Dhamodharan and Wadsworth, 1995). This dynamic localization of CLIP-170 to growing microtubule ends could occur either by transport or by treadmilling. Since speckles along the fluorescent stretch remained immobile as the fluorescence signal followed the growing microtubule ends, we concluded that CLIP-170 treadmills on the peripheral segment of growing microtubules.

We favor the following two models, which are not mutually exclusive, to explain CLIP-170 treadmilling. In the first, a particular phosphorylated form of CLIP-170 (see Rickard and Kreis, 1996) would bind specifically to the surface of a structurally distinct segment of elongating tubulin polymer. Alternatively, in the second model, CLIP-170 could associate with growing microtubules by copolymerization with tubulin. In both models, CLIP-170 subsequently dissociates from polymer as tubulin undergoes conformational changes following polymerization, ensuing GTP hydrolysis, and phosphate release, or as the polymer changes its structure upon formation of a mature microtubule. We propose that CLIP-170 must be capable of recognizing a conformational or structural difference between, on the one hand, tubulin primed to polymerize or elongating polymer, and, on the other hand, the rest of the tubulin pool. It is attractive to speculate that, owing to a higher affinity for the GTP-tubulin conformation, CLIP-170 may incorporate into or bind specifically to a cap of GTP-tubulin present at the extremity of polymerizing microtubules (Carlier and Pantaloni, 1981; Mitchison and Kirschner, 1984). Interestingly, α-tubulin folding cofactors bearing one CLIP-170-related microtubule binding domain (cofactors B and E; Tian et al., 1996, 1997) may be capable of specifically interacting with the GTP-tubulin (Lewis and Cowan, 1998). In addition, a GTP conformation–dependent interaction of tubulin with kinetochores in vitro has been described (Severin et al., 1997). This is particularly interesting, since evidence for CLIP-170 at prometaphase kinetochores has recently been obtained (Dujardin et al., 1998).

We assume that if CLIP-170 bound to polymerized segments of growing microtubule ends, it should not be restricted to the GTP-tubulin caps alone; these structures are most likely significantly smaller than the actual size of the GFP-CLIP170 dashes observed in vivo (discussed by Drechsel and Kirschner, 1994; Caplow and Shanks, 1996; Desai and Mitchison, 1997). In addition, in vitro studies did not reveal preferential binding of CLIP-170 to GTP analog–containing microtubules (Diamantopoulos et al., 1999). CLIP-170 should then, rather than detecting a conformational change at the tubulin level during polymerization, recognize a specific structural feature at the polymer level. Indeed, it has been observed in vitro that tubulin polymerizes in sheets, which subsequently close up to form a tube (Chrétien et al., 1995). Closing of the tube would then trigger dissociation of CLIP-170, perhaps reinforced by simultaneous activation of a CLIP-170 kinase. While there is so far no evidence that tubulin sheets exist on growing microtubule ends in vivo, such sheets might be sufficiently long to accommodate CLIP-170. In this context, it is interesting to note that the treadmilling of CLIP-170 is regulated by variation in both the extension and the detachment rate. The mechanism of release of CLIP-170 from older parts of microtubules may thus be regulated by a stochastic-like event. This is in agreement with the model for tubulin polymerization proposed by Chrétien et al. (1995), according to which closing of the tube is occurring at a variable rate, in a stochastic manner, due to slow conformational changes of assembled tubulin. However, in contrast with these in vitro observations, extension rate in vivo seems also to be driven by a stochastic-like mechanism, which may be due to problems in accessibility of free tubulin subunits or to more direct regulation of microtubule assembly. Considering the available data, we thus assume that CLIP-170 binds to, or coassembles into, a structurally distinct stretch of polymerized tubulin on growing microtubules. Subsequent delayed conformational and structural changes of this segment of polymerized tubulin—possibly in tandem with phosphorylation of CLIP-170—then release CLIP-170 and prevent it from binding to the rest of the (older) microtubule. In vitro binding experiments with CLIP-170 of defined phosphorylation states and microtubules with tubulin held in distinct conformations by nucleotide analogs, or defined mutations, may help to further investigate this hypothesis.

The dynamic properties of CLIP-170 in vivo may hint at interesting functional properties of the protein. On the one hand, CLIP-170 may regulate the dynamics of tubulin polymerization. In vitro experiments indicate that CLIP-170 interacts with small tubulin oligomers and stimulates microtubule polymerization (Diamantopoulos et al., 1999). CLIP-170 could thus stimulate polymerization of tubulin at plus ends either by stabilization or by cooperatively recruiting CLIP-170-tubulin oligomers in a way similar to that proposed for XMAP310 (Andersen and Karsenti, 1997).

The dynamic distribution of CLIP-170, on the other hand, has interesting implications for a putative role of CLIP-170 in microtubule-directed movement of endosomes and other particles in a cell. Since it treadmills on growing microtubule ends, its activity cruises on dynamic microtubules throughout the cytoplasm and thus continuously explores the cytoplasmic space. Interestingly, it has recently been proposed that dynamic microtubules may be preferentially used by cytoplasmic dynein (Mimin, 1997). In addition, it has been shown that CLIP-170 mediates interaction of endosomes with microtubules in vitro (Pierre et al., 1992), and more recently that it is associated with prometaphase kinetochores (Dujardin et al., 1998). Thus, CLIP-170 could be a capturing device, comparable to the “Tip Attachment Complex” (Waterman-Storer et al., 1995b; Waterman-Storer and Salmon, 1998b), establishing an initial contact between a particle and a microtubule. Once CLIP-170 has docked cargo to a track for movement, it may hand this cargo over to cytoplasmic dynein for transport. Evidence for an interaction of the dynactin complex, the

activator of cytoplasmic dynein, with CLIP-170 has indeed recently been obtained (C. Valetti et al., submitted). That growing microtubules could thus be preferred for capturing cargo is particularly interesting, since this may be part of a feedback mechanism regulating microtubule dynamic properties and their spatial arrangement. A microtubule may become transiently stabilized by tethering cargo via CLIP-170 to its dynamic end and by the subsequent interactions with dynactin and cytoplasmic dynein. An accumulation of such events may then indirectly lead to preferential growth of microtubules toward areas of a cell generating cargo at higher frequency—for example, the differentiating growth cone, a leading edge of a motile fibroblast, or the site of interaction between a killer cell and its target (Geiger et al., 1982; Kupfer et al., 1982; Vega and Solomon, 1997). The dynamic properties reported here for GFP-CLIP170, highlighting growing microtubule ends in vivo, will stimulate further studies both on the regulation of microtubule dynamics, since for the first time growth of microtubules can now be visualized specifically and directly in living cells, and on the role of CLIP-170 in regulating transport along microtubules.

Experimental Procedures

Cell Culture and Microinjection

HeLa and Vero cells were grown in GIBCO BRL culture media as described (Kreis and Lodish, 1986; Rickard and Kreis, 1990). Taxol (Paclitaxel) was a gift of the Drug Synthesis and Chemistry Branch, Developmental Therapeutics Program, Division of Cancer Treatment, National Cancer Institute (Bethesda, MD). Nocodazole (Sigma Chemical) and taxol were stored as 10 mM stock solutions in DMSO at −20°C.

Cells were grown on glass-bottomed dishes (MatTek, Ashland, MA) for microinjection. Glass capillary microinjection of DNA (50 ng/μl) or Rh-tubulin (1 mg/ml) into the nucleus or the cytoplasm of cells, respectively, was performed with an automated microinjection system (Zeiss, Switzerland) as previously described (Pepperkok et al., 1993). To avoid overexpression of recombinant protein, cycloheximide (100 μg/ml) was added 3 hr after injection.

Antibodies and Immunofluorescence

Cells were fixed at −20°C in methanol for 4 min and labeled for immunofluorescence using either of the following antibodies: monoclonal (Clontech) or polyclonal (a gift from K. Sawin) antibodies against GFP, and monoclonal antibodies against α-tubulin (1A2; Kreis, 1987) or CLIP-170 (4D3 and 2D6; Rickard and Kreis, 1991). Secondary antibodies directed against rabbit or mouse IgG (Cappel) were labeled with rhodamine or fluorescein as described (Allan and Kreis, 1986).

Preparation of Rh-Tubulin

Tubulin was purified and labeled with rhodamine (Rh-tubulin) using 5-(and 6)-carboxy-X-rhodamine succinimidyl ester (Molecular Probes) as described by Hyman et al. (1991) and stored in liquid nitrogen in the GDP-bound form. GTP was added immediately after thawing, and Rh-tubulin was then diluted to 1 mg/ml in microinjection buffer (50 mM potassium glutamate, 0.5 mM glutamic acid, and 0.5 mM $MgCl_2$ [pH 6.5]) and cleared from aggregates by centrifugation at 50,000 rpm for 30 min at 4°C (Beckman TFT 80.4 rotor) before microinjection.

Plasmid Construction

The coding sequence of a bright, red-shifted GFP mutant (S65A, V68L, S72A; Cormack et al., 1996) from plasmid pCNG2 (Shima et al., 1997) was amplified by PCR using Pfu Taq polymerase (Pharmacia) to add an AseI site before and after the GFP sequence in the correct frame. It was then inserted at the NdeI site present between the Myc tag and CLIP-170 sequence in the pGEM-Myc-CLIP-170 construct described in Pierre et al. (1994). The pCB6-GFP-CLIP170 vector was constructed by subcloning the chimeric sequence as an EcoRI insert into a modified pCB6 vector containing an EcoRI site. The pCB6-GFP-CLIP170-ΔT and pCB6-GFP-H-CLIP170 were constructed by deleting from the internal XhoI site or BglII site, respectively (corresponding to G-H-CLIP-170 and M-CLIP-170 CΔ1240, described by Pierre et al., 1994). GFP-MAP4m was constructed by amplifying the microtubule binding domain of MAP4 (amino acids 823–1176, isoform III; Chapin et al., 1995) and inserting it in frame downstream of the Myc-GFP sequence in pCB6. The sequence of the amplified fragment as well as the junctions of the different constructs were confirmed by T7 polymerase dideoxy sequencing (Pharmacia). DNA was prepared using Quiagen (Diagen) columns.

Time-Lapse Fluorescent Microscopy and Speed Quantitation

Cells on glass-bottomed dishes were placed into prewarmed Hank's/BSA medium (100 mM HEPES, 137 mM NaCl, 5.4 mM KCl, 1.3 mM $CaCl_2$, 1 mM $MgCl_2$, and 5.5 mM glucose [pH 7.4] containing 0.5% BSA) and observed at 37°C using an inverted fluorescence microscope (Zeiss Axiovert TV135, ×100 planapo objective), essentially as previously described (Scales et al., 1997). For drug treatment and subsequent washout experiments, the incubation medium was directly changed in the incubation chamber on the microscope stage without interruption of the recording. Excitation light was usually attenuated to 13%–50% to minimize photodamage. For covisualization of Rh-tubulin and GFP-CLIP170, we used the FITC filters for GFP and the Cy3 filter for rhodamine; filters were manually switched between each successive image acquisition. Signals of images were recorded, and movies assembled, using the software package IPLab spectrum V3.1 for 0.4 s every 2–5 s using a cooled CCD camera (Photometrics CH250, 1317 × 1035 pixels) controlled by a Power Macintosh 8100/100. Mean velocities of extension were determined by tracking the tip of selected GFP-CLIP170-positive structures and measurement of its displacement as a function of time. Only dashes that could be clearly followed for at least seven frames were analyzed. For coanalysis of stretch length, and extension and detachment speed, tip and tail of the comet-like staining were tracked and their speed of displacement plotted on a graph. The mean values calculated in this case are not computed per microtubule using different cells as before but using the different displacements tracked within a cell. Data are presented in the text as mean values ± standard error. Images and data were processed using Adobe Photoshop 3.0 and Cricket Graph 3.0 software, respectively. Movies in QuickTime format are accessible through the web at http://www.cell.com/supplemental/ and at http://www.unige.ch/kreis-lab/.

Acknowledgments

We would like to thank Drs. B. Cormack and D. Shima for the GFP cDNA, Dr. K. Sawin for antibodies against GFP, Dr. C. Bulinski for the MAP4 cDNA, the Kreis lab for stimulating discussions, and Drs. Holly V. Goodson, Eric Karsenti, and Anthony A. Hyman for valuable suggestions on the manuscript. G. S. D. was supported by a grant from Fonds National Suisse attributed to Dr. J. E. Rickard. This research was supported by a grant to T. E. K. from the Fonds Nationale Suisse and by the Canton de Genève.

Received August 31, 1998; revised December 21, 1998.

References

Allan, V.J., and Kreis, T.E. (1986). A microtubule-binding protein associated with membranes of the Golgi apparatus. J. Cell Biol. *103*, 2229–2239.

Andersen, S.S.L., and Karsenti, E. (1997). XMAP310: a Xenopus rescue-promoting factor localized to the mitotic spindle. J. Cell Biol. *139*, 975–983.

Belmont, L.D., and Mitchison, T.J. (1996). Identification of a protein that interacts with tubulin dimers and increases the catastrophe rate of microtubules. Cell *84*, 623–631.

Bloom, G.S., and Goldstein, L.S. (1998). Cruising along microtubule highways: how membranes move through the secretory pathway. J. Cell Biol. *140*, 1277–1280.

Caplow, M. (1992). Microtubule dynamics. Curr. Opin. Cell Biol. *4*, 58–65.

Caplow, M., and Shanks, J. (1996). Evidence that a single monolayer tubulin-GTP cap is both necessary and sufficient to stabilize microtubules. Mol. Biol. Cell *7*, 663–675.

Carlier, M.F., and Pantaloni, D. (1981). Kinetic analysis of guanosine 5′-triphosphate hydrolysis associated with tubulin polymerization. Biochemistry *20*, 1918–1924.

Cassimeris, L., Pryer, N.K., and Salmon, E.D. (1988). Real-time observations of microtubule dynamic instability in living cells. J. Cell Biol. *107*, 2223–2231.

Chapin, S.J., Lue, C.M., Yu, M.T., and Bulinski, J.C. (1995). Differential expression of alternatively spliced forms of MAP4: a repertoire of structurally different microtubule-binding domains. Biochemistry *34*, 2289–2301.

Charrasse, S., Schroeder, M., Gauthier-Rouviere, C., Ango, F., Cassimeris, L., Gard, D.L., and Larroque, C. (1998). The TOGp protein is a new human microtubule-associated protein homologous to the Xenopus XMAP215. J. Cell Sci. *111*, 1371–1383.

Chrétien, D., Fuller, S.D., and Karsenti, E. (1995). Structure of growing microtubule ends: two-dimensional sheets close into tubes at variable rates. J. Cell Biol. *129*, 1311–1328.

Cole, N.B., and Lippincott-Schwartz, J. (1995). Organization of organelles and membrane traffic by microtubules. Curr. Opin. Cell Biol. *7*, 55–64.

Cormack, B.P., Valdivia, R.H., and Falkow, S. (1996). FACS-optimized mutants of the green-fluorescent protein (GFP). Gene *170*, 33–38.

Desai, A., and Mitchison, T.J. (1997). Microtubule polymerization dynamics. Annu. Rev. Cell. Dev. Biol. *13*, 83–117.

Dhamodharan, R., and Wadsworth, P. (1995). Modulation of microtubule dynamic instability in vivo by brain microtubule associated proteins. J. Cell Sci. *108*, 1679–1689.

Diamantopoulos, G.D., Perez, F., Goodson, H.V., Batelier, G., Melki, R., Kreis, T.E., and Rickard, J.E. (1999). Dynamic localization of CLIP-170 to microtubule plus ends is coupled to microtubule assembly. J. Cell Biol. *144*, 99–112.

Drechsel, D.N., and Kirschner, M.W. (1994). The minimum GTP cap required to stabilize microtubules. Curr. Biol. *4*, 1053–1061.

Dujardin, D., Wacker, U.I., Moreau, A., Schroer, T.A., Rickard, J.E., and De Mey, J.R. (1998). Evidence for a role of CLIP-170 in the establishment of metaphase chromosome alignment. J. Cell Biol. *141*, 849–862.

Gard, D.W., and Kirschner, M.W. (1987). A microtubule-associated protein from *Xenopus* eggs that specifically promotes assembly at the plus-end. J. Cell Biol. *105*, 2203–2215.

Geiger, B., Rosen, D., and Berke, G. (1982). Spatial relationships of microtubule-organizing centers and the contact area of cytotoxic T lymphocytes and target cells. J. Cell Biol. *95*, 137–143.

Goodson, H.V., Valetti, C., and Kreis, T.E. (1997). Motors and membrane traffic. Curr. Opin. Cell Biol. *9*, 18–28.

Hirokawa, N. (1998). Kinesin and dynein superfamily proteins and the mechanism of organelle transport. Science *279*, 519–526.

Holzbaur, E.L.F., Hammarback, J.A., Paschal, B.M., Kravit, N.G., Pfister, K.K., and Vallee, R.B. (1991). Homology of a 150K cytoplasmic dynein-associated polypeptide with the *Drosophila* gene *Glued*. Nature *351*, 579–583.

Hyman, A.A., and Karsenti, E. (1996). Morphogenetic properties of microtubules and mitotic spindle assembly. Cell *84*, 401–410.

Hyman, A.A., Salser, S., Drechsel, D.N., Unwin, N., and Mitchison, T.J. (1992). Role of GTP hydrolysis in microtubule dynamics: information from a slowly hydrolyzable analogue, GMPCPP. Mol. Biol. Cell *3*, 1155–1167.

Kirschner, M., and Mitchison, T. (1986). Beyond self-assembly: from microtubules to morphogenesis. Cell *45*, 329–342.

Kreis, T.E. (1987). Microtubules containing detyrosinated tubulin are less dynamic. EMBO J. *6*, 2597–2606.

Kreis, T.E., and Lodish, H.F. (1986). Oligomerization is essential for transport of vesicular stomatitis viral glycoprotein to the cell surface. Cell *46*, 929–937.

Kupfer, A., Louvard, D., and Singer, S.J. (1982). Polarization of the Golgi apparatus and the microtubule-organizing center in cultured fibroblasts at the edge of an experimental wound. Proc. Natl. Acad. Sci. USA *79*, 2603–2607.

Lewis, S.A., and Cowan, N.J. (1998). The α and β-tubulin folding pathways. Trends Cell Biol. *7*, 479–484.

Mandelkow, E.-M., Mandelkow, E., and Milligan, R.A. (1991). Microtubule dynamics and microtubule caps: a time-resolved cryo-electron microscopy study. J. Cell Biol. *114*, 977–991.

Marklund, U., Larsson, N., Melander Gradin, H., Brattsand, G., and Gullberg, M. (1996). Oncoprotein 18 is a phosphorylation-responsive regulator of microtubule dynamics. EMBO J. *15*, 5290–5298.

Mata, J., and Nurse, P. (1997). tea1 and the microtubular cytoskeleton are important for generating global spatial order within the fission yeast cell. Cell *89*, 939–949.

Mimin, A.A. (1997). Dispersal of Golgi apparatus in nocodazole-treated fibroblasts is a kinesin-driven process. J. Cell Sci. *110*, 2495–2505.

Mitchison, T.J., and Kirschner, M. (1984). Dynamic instability of microtubule growth. Nature *312*, 237–242.

Näthke, I.S., Adams, C.L., Polakis, P., Sellin, J.H., and Nelson, W.J. (1996). The adenomatous polyposis coli tumor suppressor protein localizes to plasma membrane sites involved in active cell migration. J. Cell Biol. *134*, 165–179.

Pepperkok, R., Schell, J., Horstmann, H., Hauri, H.P., Griffiths, G., and Kreis, T.E. (1993). β-COP is essential for biosynthetic membrane transport from the endoplasmic reticulum to the Golgi complex in vivo. Cell *74*, 71–82.

Pierre, P., Scheel, J., Rickard, J.E., and Kreis, T.E. (1992). CLIP-170 links endocytic vesicles to microtubules. Cell *70*, 887–900.

Pierre, P., Pepperkok, R., and Kreis, T.E. (1994). Molecular characterization of two functional domains of CLIP-170 in vivo. J. Cell Sci. *107*, 1909–1920.

Rickard, J.E., and Kreis, T.E. (1990). Identification of a novel nucleotide-sensitive microtubule-binding protein in HeLa cells. J. Cell Biol. *110*, 1623–1633.

Rickard, J.E., and Kreis, T.E. (1991). Binding of pp170 to microtubules is regulated by phosphorylation. J. Biol. Chem. *266*, 17597–17605.

Rickard, J.E., and Kreis, T.E. (1996). CLIPs for organelle-microtubule interactions. Trends Cell Biol. *6*, 178–183.

Sammak, P.J., and Borisy, G.G. (1988). Direct observation of microtubule dynamics in living cells. Nature *332*, 724–726.

Scales, S.J., Pepperkok, R., and Kreis, T.E. (1997). Visualization of ER-to-Golgi transport in living cells reveals a sequential mode of action for COPII and COPI. Cell *90*, 1137–1148.

Schroer, T.A., and Sheetz, M.P. (1991). Two activators of microtubule-based vesicle transport. J. Cell Biol. *115*, 1309–1318.

Severin, F.F., Sorger, P.K., and Hyman, A.A. (1997). Kinetochores distinguish GTP from GDP forms of the microtubule lattice. Nature *388*, 888–891.

Shima, D.T., Haldar, K., Pepperkok, R., Watson, R., and Warren, G. (1997). Partitioning of the Golgi apparatus during mitosis in living HeLa cells. J. Cell Biol. *137*, 1211–1228.

Simon, J.R., and Salmon, E.D. (1990). The structure of microtubule ends during the elongation and shortening phases of dynamic instability examined by negative-stain electron microscopy. J. Cell Sci. *96*, 571–582.

Tian, G., Huang, Y., Rommelaere, H., Vandekerckhove, J., Ampe, C., and Cowan, N.J. (1996). Pathway leading to correctly folded β-tubulin. Cell *86*, 287–296.

Tian, G., Lewis, S.A., Feierbach, B., Stearns, T., Rommelaere, H., Ampe, C., and Cowan, N.J. (1997). Tubulin subunits exist in an activated conformational state generated and maintained by protein cofactors. J. Cell Biol. *138*, 821–832.

Vale, R.D. (1999). Molecular motors and associated proteins. In

Guidebook to the Cytoskelatal and Motor Proteins, T.E. Kreis and R.D. Vale, eds. (Oxford: Oxford University Press), in press.

Vasquez, R.J., Gard, D.L., and Cassimeris, L. (1994). XMAP from Xenopus eggs promotes rapid plus end assembly of microtubules and rapid microtubule polymer turnover. J. Cell Biol. *127*, 985–993.

Vega, L.R., and Solomon, F. (1997). Microtubule function in morphological differentiation: growth zones and growth cones. Cell *89*, 825–828.

Walczak, C.E., Mitchison, T.J., and Desai, A. (1996). XKCM1: a Xenopus kinesin-related protein that regulates microtubule dynamics during mitotic spindle assembly. Cell *84*, 37–47.

Walker, R.A., O'Brien, E.T., Pryer, N.K., Soboeiro, M.F., Voter, W.A., Erickson, H.P., and Salmon, E.D. (1988). Dynamic instability of individual microtubules analyzed by video light-microscopy—rate constants and transition frequencies. J. Cell Biol. *107*, 1437–1448.

Waterman-Storer, C.M., and Salmon, E.D. (1997). Actomyosin-based retrograde flow of microtubules in the lamella of migrating epithelial cells influences microtubule dynamic instability and turnover and is associated with microtubule breakage and treadmilling. J. Cell Biol. *139*, 417–434.

Waterman-Storer, C.M., and Salmon, E.D. (1998a). How microtubules get fluorescent speckles. Biophys. J. *75*, 2059–2069.

Waterman-Storer, C.M., and Salmon, E.D. (1998b). Endoplasmic reticulum membrane tubules are distributed by microtubules in living cells using three distinct mechanisms. Curr. Biol. *8*, 798–806.

Waterman-Storer, C.M., Karki, S., and Holzbaur, E.L. (1995a). The $p150^{Glued}$ component of the dynactin complex binds to both microtubules and the actin-related protein centractin (Arp-1). Proc. Natl. Acad. Sci. USA *92*, 1634–1638.

Waterman-Storer, C.M., Gregory, J., Parsons, S.F., and Salmon, E.D. (1995b). Membrane/microtubule tip attachment complexes (TACs) allow the assembly dynamics of plus ends to push and pull membranes into tubulovesicular networks in interphase Xenopus egg extracts. J. Cell Biol. *130*, 1161–1169.

Wilson, L., and Jordan, M.A. (1994). Pharmacological probes of microtubule function. In Microtubules, J.S. Hyams and C.W. Lloyd, eds. (New York: Wiley-Liss), pp. 59–83.